High hardness and low dielectric constant thin films with oriented urea oligomers by physical vapor deposition

Morimoto, Masahiro
Fukutomi, Tatsuya
Koshiba, Yasuko
Ishida, Kenji

(Citation)
Journal of Materials Science, 54(3):2483-2492

(Issue Date)
2019-02

(Resource Type)
journal article

(Version)
Accepted Manuscript

(URL)
https://hdl.handle.net/20.500.14094/90006459

High Hardness and Low Dielectric Constant Thin Films with Oriented Urea Oligomers by Physical Vapor Deposition

*Masahito Morimoto[1,2]
[1]Department of Chemical Science & Engineering, Graduate School of Engineering, Kobe University, Rokkodai 1-1, Nada, Kobe, 657-8501, Japan
[2]Graduate School of Science & Engineering for Research, University of Toyama, 3190 Gofuku, Toyama, 930-8555, Japan
Email: morimoto@eng.u-toyama.ac.jp, Tel: +81-76-445-6734
ORCID: 0000-0002-1156-6494

Tatsuya Fukutomi[1],
[1]Department of Chemical Science & Engineering, Graduate School of Engineering, Kobe University, Rokkodai 1-1, Nada, Kobe, 657-8501, Japan
Email: ta2co.116@gmail.com

Yasuko Koshiba[1],
[1]Department of Chemical Science & Engineering, Graduate School of Engineering, Kobe University, Rokkodai 1-1, Nada, Kobe, 657-8501, Japan
Email: koshiba@kobe-u.ac.jp
ORCID: 0000-0001-7189-0109

Kenji Ishida[1]
[1]Department of Chemical Science & Engineering, Graduate School of Engineering, Kobe University, Rokkodai 1-1, Nada, Kobe, 657-8501, Japan
Email: kishida@crystal.kobe-u.ac.jp
ORCID: 0000-0003-1227-9638

***CORRESPONDING AUTHOR**
Masahiro Morimoto
Graduate School of Science & Engineering for Research, University of Toyama, 3190 Gofuku, Toyama, 930-8555, Japan
Email: morimoto@eng.u-toyama.ac.jp, Tel: +81-76-445-6734

Oligomer of undecylurea (OUA11) thin films with a high crystallinity, surface hardness, perpendicular orientation, and low dielectric constant were fabricated by physical vapor deposition. The thin films were composed of single OUA11, which has a relatively high molecular weight (Mw: 2500, Mn: 1200) and could be vapor-deposited without thermal decomposition. These films had a much higher crystallinity, and a high surface hardness level of 9H in the pencil hardness test. The dielectric constant of the OUA11 films is estimated to be 2.1–2.3 in the frequency range of 1 Hz to 0.1 MHz, which is lower than that of typical low dielectric constant (low-k) materials. These physical and electrical properties are caused by the unique structure with the molecular dipoles oriented parallel to the electrodes on the substrate and the strong intermolecular hydrogen bonds. The unique structure could not be observed with spin-coating and is specific to the vapor-deposited films. We expect that the OUA11 films with a high hardness and a low dielectric constant can be used not only as protective coatings but also as electronic materials.
KEYWORDS: urea oligomer, vapor-deposited films, dielectric constant, molecular orientation, hydrogen bonds

INTRODUCTION

Urea materials form durable hydrogen bonds and show interesting material properties. Polymeric materials that include urea groups, e.g., polyureas, exhibit good resistance to water, chemicals, and thermal effects [1–3]. Their derivatives have been used as water-, thermal-, and impact-resistant protective coatings [4–6]. In addition, they have good piezo-[7,8], pyro-[9–11] and ferro-electric [12,13] properties because of the large dipole moment of the urea bond (NHC=ONH) (4.9 D) [14], which is more than double that of the typical ferroelectric polymer, poly(vinylidene fluoride/trifluoroethylene) (2.1 D). Hence, these materials are expected to be novel and durable organic electronic materials.

Control over the orientation of intermolecular dipoles of polyurea in the films is necessary for the effective use of the electrical properties. Moreover, it is important for the polyurea films to be thin so that low applied voltages can be used to align the molecular dipoles; however, these goals have been quite challenging to achieve [15]. It is difficult to control the molecular orientation and crystallinity, especially in a wet-process, because of the large molecular weight and strong hydrogen bonds in polyureas. Our previous studies reported that the polyurea thin films prepared by a spin-coating method had a low crystallinity [11,15]. On the other hand, organic thin films have been fabricated by physical vapor deposition (PVD). PVD can be used to control the molecular orientation and crystallinity because it has a low contamination and an easily controllable deposition rate. PVD is a technique to deposit thin films on a substrate by evaporating the source material under vacuum; thus, this form of thin films has a good chemical purity without solvent effects and a voluntary thickness. Several organic thin films and their structural controlling effects have already been reported by some researchers [16–18]. Aliphatic chain materials form highly crystalline and oriented thin films, and their characterization is dependent on the substrate temperature, substrate materials and the deposition rate in the vapor deposition [19–23]. The relationships between the physical structure and the electrical characteristics have been shown for aromatic materials [24–27]. These researchers used low molecular weight materials that can be deposited by vapor deposition, but polymers cannot be deposited in vacuum without thermal decomposition [28]. It is necessary to optimize the molecular weight to achieve the chemically pure and highly crystalline thin films.

Therefore, to improve the purity, the crystallinity and the molecular orientation, oligomer of undecylurea (OUA11) thin films have been prepared by PVD technique with an optimum molecular weight. The surface hardness and the structural and the dielectric properties of OUA11 films have been investigated and compared with spin-coated OUA11 films.

EXPERIMENTAL

OUA11 materials and film preparation

The oligomer of undecylurea (OUA11, Mw: 2500, Mn: 1200) and the polyundecylurea (PUA11, Mw: 13000, Mn: 7000) consisting of undecylurea were supplied by Unitika Limited. PUA11 was synthesized from carbon dioxide and [1,11]-diaminoundecane and had a linear structure with polar urea (NHC=ONH) and alkyl (–(CH2)n–) components.

The OUA11 thin film was deposited on plain and Al-coated Si substrates by PVD technique at 25 °C (where the Al serves as a bottom electrode). The plain Si substrates were used for X-ray diffraction (XRD) measurement and Fourier transform infrared (FT-IR) transmission method, and the Al-coated Si substrates were used for FT-IR reflection absorption spectroscopy (RAS) method and dielectric spectroscopy. The chamber was initially evacuated to 5×10^{-4} Pa. According to TG results, at first, the source temperature was raised to 220 °C. After the evaporation rate reached zero, the source temperature was increased again to up to 230 °C, and the shutter was open to start the deposition of OUA11 films. The evaporation rate was maintained within the range of 0.6-1.2 nm/min. The film thickness was measured to be 500 nm by a controlled quartz-crystal. The melting points of the vapor-deposited OUA11 films and the powder sample were measured by differential scanning calorimetry (DSC) to evaluate the thermal decomposition rate. The DSC curves were measured at a heating rate of 10 °C/min using a Seiko Instruments Inc. EXSTAR 6000 under a normal atmosphere. As a reference sample, OUA11 was dissolved in 4.0 wt% hexafluoroisopropylalcohol (HFIP) and spin-coated at 2500 rpm for 30 s under N2 at

25 °C. The spin-coated OUA11 films were annealed at 220 °C for 30 s under a N2 environment and then cooled at a rate of 1.0 °C/min. The thickness of the spin-coated OUA11 films were found to be 500–600 nm using a stylus profiler (AMBiOS Technology XP-200).

Film structure, thermal and electrical measurements

The thermal properties of OUA11 and PUA11 powder samples were measured by thermogravimetry (TG) at a heating rate of 5 °C/min under a vacuum of 5×10^{-3} Pa using custom-designed systems. The melting points of the vapor-deposited OUA11 films and the powder sample were measured by DSC to evaluate the thermal decomposition rate. The DSC curves were measured at a heating rate of 10 °C/min using a Seiko Instruments Inc. EXSTAR 6000 under a normal atmosphere.

The surface morphological properties of vapor-deposited and spin-coated OUA11 films were measured by an atomic force microscope (AFM) (JOEL JSPM-5200) in a tapping mode; the scanning area is 5 × 5 µm, and the scan speed is 1.0 ms/point. Si cantilevers (Olympus) with resonant frequencies of ~300 kHz and spring constants of ~42 N/m were used. The structural analysis was performed by out-of-plane XRD patterns on a Rigaku Ultima IV Protectus instrument operated at 40 kV and 40 mA with Cu-Kα radiation. The FT-IR transmission and RAS spectra were also measured under a vacuum of ~1.0 Pa using a JASCO FT/IR-660Plus instrument. The resolution and the cumulative number of measurements were 4 cm^{-1} and 512 cycles, respectively.

To evaluate the electrical properties of the vapor-deposited OUA11 films, Al/OUA11/Al capacitors were fabricated. Both top and bottom Al electrodes were vapor-deposited by thermal evaporation technique; the thickness was maintained at a constant of 100 nm in each case. The dielectric spectra were measured by applying an AC voltage of 0.1 V under a vacuum of 5×10^{-2} Pa. The measured frequency were 0.01 to 10^5 Hz and the temperature range were 25 to 123 °C. The dielectric spectra measurement system was constituted from a solartron dielectric interface 1296 and an impedance analyzer 1260 by TOYO Corporation.

RESULTS AND DISCUSSION

Thermo-physical properties of OUA11

Fig. 1 shows the TG curves of PUA11 and OUA11 powder samples at a heating rate of 5 °C/min under a vacuum of 5×10^{-3} Pa. The TG curve of PUA11 exhibits a one-step weight loss, starting at a temperature above 300 °C and ending at a temperature of 360 °C. This indicates that the thermal decomposition of PUA11 molecules [29,30] happened within the temperature range of 300-360 °C. In contrast, the TG curve of OUA11 exhibits three steps of weight loss. In the first step, the weight of OUA11 gradually decreases between 110 and 220 °C. It continues to decrease slowly with increasing temperature until up to 300 °C in the second step, and third, the weight of OUA11 drastically decreases above 300 °C. This probably indicates that the first step of weight loss can be attributed to the sublimation of low molecular weight components in the original powder sample. The second weight-loss step can be attributed to the sublimation of the remaining high molecular weight components. The molecules are evaporated in this step to form the vapor-deposited OUA11 films. The third weight-loss step is observed above 300 °C, indicating the thermal decomposition of OUA11 molecules. The two TG curves at ~350 °C are coincident, which indicates the thermal decomposition of OUA11 and PUA11. If the weight loss means the sublimation, the two temperatures should be different due to the molecular weight.

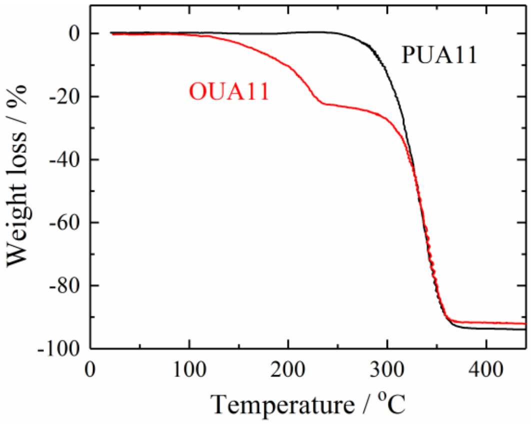

Fig. 1 TG curves of PUA11 (black line) and OUA11 (red line) at a heating rate of 5 °C/min under a vacuum of 5×10^{-3} Pa.

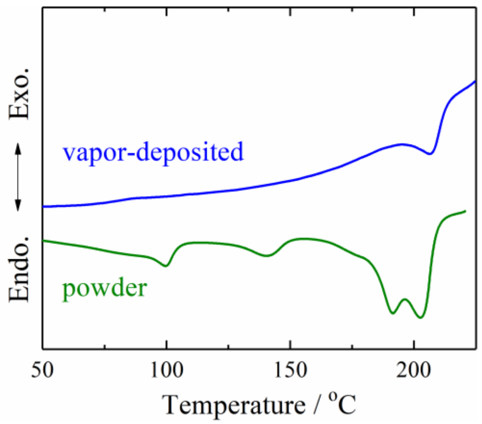

Fig. 2 DSC curves of the vapor-deposited OUA11 films (blue line) and the powder sample (green line) at a heating rate of 10 °C/min.

Subsequently, the thermal property of the original powder OUA11 sample is compared with the OUA11 films vapor-deposited at 230 °C following the second step of the TG curve. Their DSC curves are shown in Fig. 2. The vapor-deposited film exhibits a single endothermic peak, while the powder sample shows several peaks. The powder sample consisted of molecules with various polymerization degrees, i.e., n = 2–12; thus, the several peaks in the DSC curve indicate the melting points corresponding to each molecular weight. In the DSC curve, the presence of only one peak suggests that the vapor-deposited OUA11 films are formed with a selectively high molecular weight. Therefore, the TG and DSC results suggest that the OUA11 sample can be refined by vacuum deposition and the vapor-deposited OUA11 films should be evaporated between 220 and 300 °C, that provides the less components i.e., the relatively narrow molecular weight distribution, than the powder sample.

Structural analysis of OUA11 films

The AFM images and the XRD patterns of the vapor-deposited and spin-coated OUA11 films are shown in Fig. 3. The vapor-deposited films are covered by a stiff rectangular-like structure with a height of 40–50 nm and a width of 700–800 nm [Fig. 3(a)]. The structure of the same size is uniformly formed on the substrate. In contrast, the spin-coated OUA11 film has many small grains, which are tinier and rounder than the structure of vapor-deposited films. The average roughness was calculated to be 25.6 nm on the vapor-deposited films and 6.05 nm on the spin-coated films. Moreover, the XRD patterns of the vapor-deposited OUA11 films have sharper peaks than those of the spin-coated films [Fig. 3(c)]. This indicates that the vapor-deposited OUA11 films are highly crystalline films and that the rectangular-like structure is the crystal grain, of which the size is estimated to be 39.4 nm according to the Scherrer equation [31]; this grain size is consistent with the grain height observed by the AFM images. The three XRD peaks of the vapor-deposited films have lattice spacings of 0.867, 0.437, and 0.293 nm; however, these peaks do not appear for the spin-coated OUA11 films and the powder OUA11 sample. The peaks of the spin-coated films and the powder sample are in good agreement with the lattice spacings, which are estimated using the expected lattice constants (a, b, c = 0.48, 0.56, 1.75 nm and α, β, γ = 49, 77, 63°) [15,32,33]; the peaks at $2\theta = 6.95°$ (1.27 nm), 21.1° (0.421 nm), and 23.4° (0.380 nm) correspond to the (001), (100), and (010) reflections, respectively. Meanwhile, the lattice spacings of the vapor-deposited films, i.e., 0.867, 0.437, and 0.293 nm, are equivalent to a half, a quarter, and a sixth of the length of the c axis (1.75 nm), respectively. This means that the molecular chains of the vapor-deposited films have been oriented perpendicularly to the substrate and have formed the highly crystalline thin films. In addition, we expect the vaper-deposited OUA11 films have formed a metastable state, whose molecular chains are perpendicularly aligned to the substrate, and the metastable state is not included in the stable state of OUA11. This is one of the reasons why the urea oligomers used in this work should show a stable triclinic state because the powder XRD pattern corresponds to the urea polymer, previously reported as the triclinic state [15, 32]. The other reason is that the metastable state of the vapor-deposited films cannot maintain at around 120 °C, e. g. the all XRD peaks of the vapor-deposited films disappeared after the annealing at 120 °C for 60 min under a nitrogen atmosphere. The metastable state of the

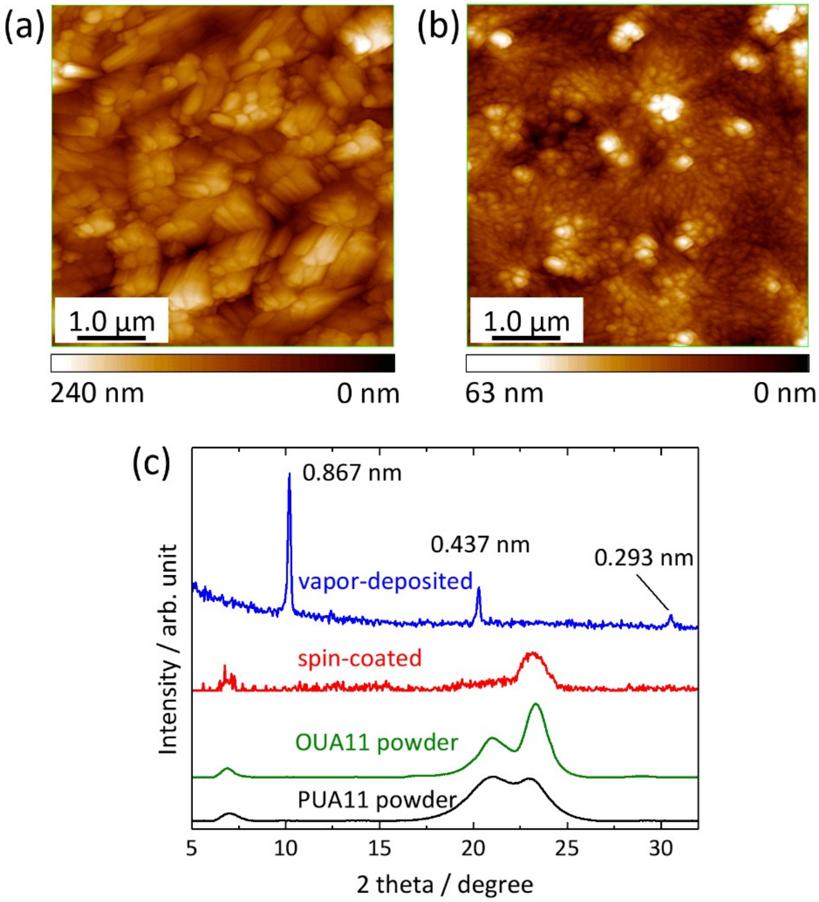

Fig. 3 Tapping mode AFM images of (a) vapor-deposited and (b) spin-coated OUA11 thin films. (c) XRD patterns of vapor-deposited (blue line), spin-coated (red line) OUA11 films, OUA11 powder (green line) and PUA11 powder (black line).

vapor-deposited OUA11 films in this work may be unique because the vapor-deposited nylon-11 films [28] are similar materials that show the XRD patterns of the vapor-deposited films correspond to the powder sample.

The FT-IR RAS spectra of the vapor-deposited and the spin-coated OUA11 films are shown in Fig. 4(a). The distinctive peaks of the vapor-deposited films are consistent with the spin-coated films. The spectrum of our vapor-deposited OUA11 films exhibits only peaks attributed to the urea oligomer; no peaks attributable to the degradation (2200–2300 cm^{-1}) are observed. Previous studies have reported that isocyanate or nitrile groups are observed, while the urea groups are thermally decomposed and polymerized in vacuum

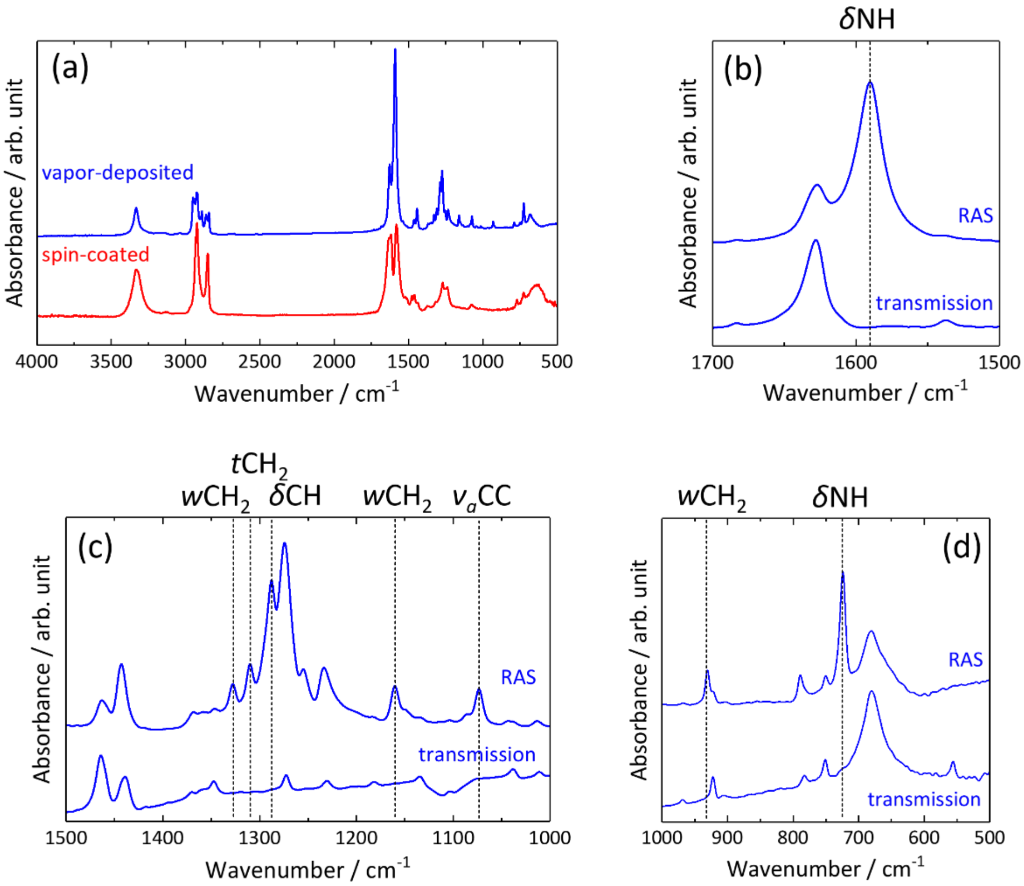

Fig. 4 (a) FT-IR RAS spectra of vapor-deposited (blue line) and spin-coated OUA11 films (red line). FT-IR RAS and transmission spectra of the vapor-deposited films (b) in the urea bond vibration region and (c, d) in the others vibration region.

[7,28,34]. Regarding the determination of molecular orientation in the vapor-deposited OUA11 thin films, the transmission and the RAS method have been used [Fig. 4(b,c,d)]. The N─H bending mode at 1588 and 724 cm^{-1}, the CH$_2$ wagging mode at 1326, 1160 and 930 cm^{-1}, the CH$_2$ twist mode at 1310 cm^{-1}, the C─H bending mode at 1288 cm^{-1}, and the C─C antisymmetric stretching mode at 1072 cm^{-1} are parallel to the molecular axis [2,18,35–40]. These peaks are observed in the RAS spectra and lost in the transmission spectra, which indicates that the orientation of the molecular chains in the vapor-deposited OUA11 films is perpendicular to the substrate, in good agreement with the XRD results. In contrast, the difference between the transmission and RAS spectra of the spin-coated

OUA11 films could not be confirmed. This is probably because the orientation of the spin-coated films becomes random or parallel to the substrate (Fig. S1). Fig. S1 in the supplementary material shows the FT-IR RAS and transmission spectra of the spin-coated OUA11 films (a) in the urea bond vibration region and (b) in the alkyl chain vibration region.

OUA11 film characteristics; Surface hardness and Dielectric properties

The surface hardness of vapor-deposited OUA11 films is measured using a pencil hardness test (ISO 15184). The hardness is estimated to be 9H, which is incredibly high and well above the usual measuring range (~6H). The high hardness of the vapor-deposited films is probably caused by the high crystallinity and the rigid intermolecular hydrogen bonds in the vapor-deposited OUA11 films. Generally, organic thin films are fragile, soft, and weak; thus, the high hardness of the OUA11 vapor-deposited films in this work could overcome this limitation, and they are expected to have wide applications as protective coatings.

The dielectric spectra of the vapor-deposited and spin-coated OUA11 films measured under a vacuum of 5 × 10^{-2} Pa are shown in Fig. 5. The relative dielectric constants of the vapor-deposited and spin-coated films were estimated to be 2.1–2.3 and 2.4–2.9 in the frequency range of 0.1 Hz to 0.1 MHz at 25 °C, respectively. Both the dielectric constants of vapor-deposited and spin-coated films are comparable to those of typical small dielectric constant (low-k) materials, such as polyethylene (2.3–3.0) [41,42], polytetrafluoroethylene (2.1–3.0) [42–44], polyimide (3.0–5.0) [42,45], and SiO2 (3.9–4.3) [41,43]. This reveals that the OUA11 thin films behave like low-k materials; moreover, the dielectric constant of vapor-deposited films did not change even at 50 °C, indicating a good thermal stability. The dielectric constant at low frequencies increases with increasing temperature, indicating that the thermally activated impurity charges behave like leakage

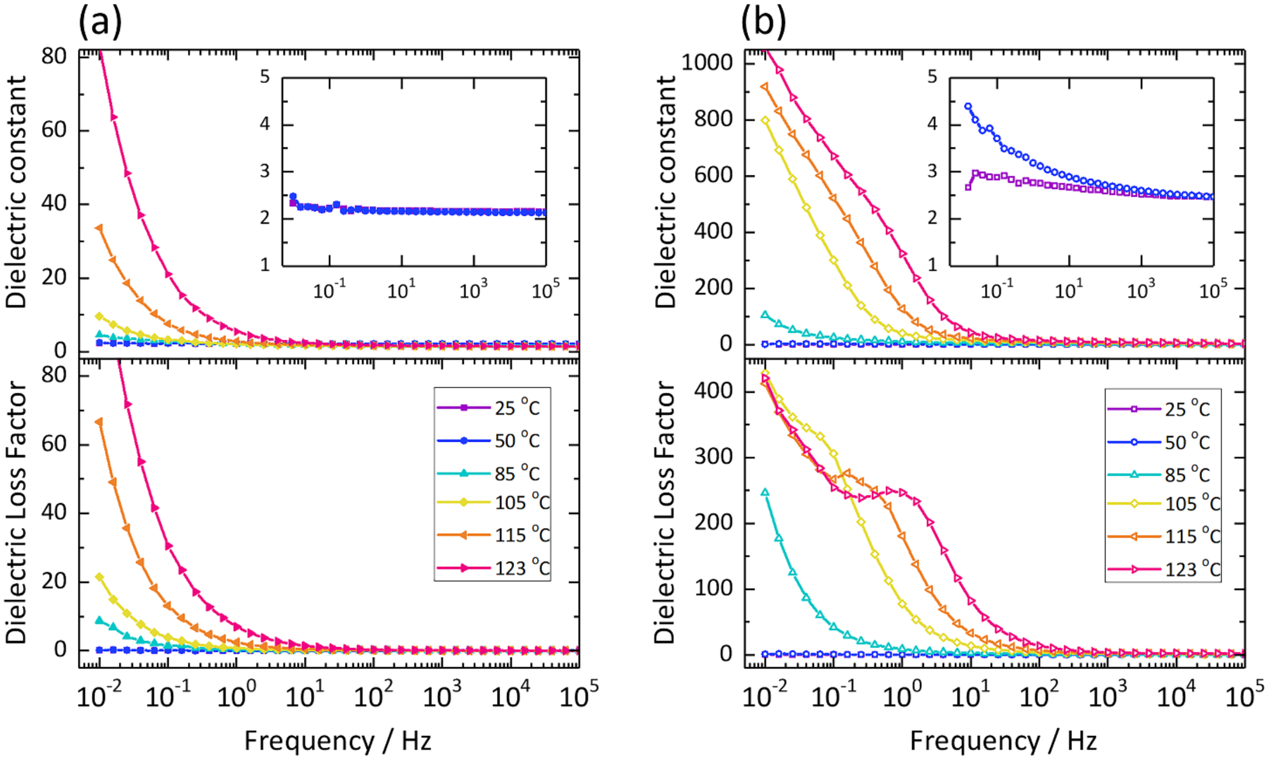

Fig. 5 Relative dielectric constant and dielectric loss factor of (a) vapor-deposited (filled symbols) and (b) spin-coated (open symbols) OUA11 films measured by applying an AC voltage of 0.1 V under a vacuum of 5 × 10^{-2} Pa. Insets show the relative dielectric constant at 25 and 50 °C.

components in the OUA11 films; moreover, the dielectric constant of the vapor-deposited films has a lower value (> 80) than that of the spin-coated films (> 1000) at 0.01 Hz and 123 °C. This means that the vapor-deposited films were protected from contamination due to the solvent and the use of a selectively high molecular weight. Above 105 °C, the peaks of dielectric loss, i.e., the dielectric relaxation, in the spin-coated films shift to higher frequencies with increasing temperature. The growth of the loss peaks suggests that the molecular dipoles of OUA11 films were activated with increasing temperature. The molecular orientation in the spin-coated films might be in a random state, and thus, the component of the dipoles perpendicular to the electrodes causes peaks to appear in the dielectric relaxation. At room temperature, urea groups form strong hydrogen bonds, which probably inhibit the fluctuation of dipoles. High temperatures cause the relaxation of hydrogen bonds and promote the fluctuation of dipoles. For the vapor-deposited OUA11 films, we did not observe any peak of dielectric loss even at high temperature. The out-of-plane dielectric constant of the vapor-deposited OUA11 films showed a significantly lower value, even though the in-plane constant parallel to the direction of the urea dipoles is expected to be high. Using an in-plane electrode, e.g., a comb type, the electrical properties of highly oriented dipoles can be exploited, and the perpendicular OUA11 films can be applied in various electronics fields.

A schematic of the vapor-deposited OUA11 films is summarized in Fig. 6. According to the experimental results, the vapor-deposited films are composed of perpendicularly oriented molecular chains to the substrate. The molecules included the dipoles due to the urea groups, which are parallel to the substrate and form the intermolecular hydrogen bonds. The vapor-deposited films have been shown to have a superior surface hardness and thermal stability of dielectric properties. Furthermore, the vapor-deposited films have a high crystallinity and are obtained with an out-of-plane lattice spacing along c axis. The unique film structure could not be observed with spin-coating, and it is a structure specific to the vapor-deposited films.

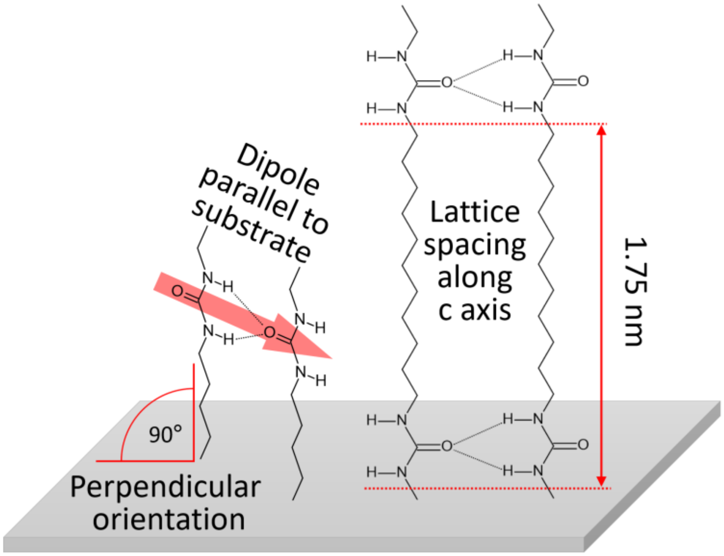

Fig. 6 Schematic of the vapor-deposited OUA11 films based on the experimental results.

Conclusion

The single OUA11 thin films were fabricated by physical vapor deposition, and their film structure and electrical properties were investigated. For TG experiments under vacuum, the weight loss of OUA11 proceeds in three steps, and the few components with the narrow molecular weight distribution selectively evaporated in the second step form the vapor-deposited OUA11 films. The crystallinity of the vapor-deposited films was higher than that of the spin-coated films, and the crystal size of the vapor-deposited films was 39.4 nm, which is identical to the height of the grains in the AFM images. However, the diffraction peaks of the vapor-deposited films could not be readily interpreted in terms of the known lattice constants of OUA11 powder, but they corresponded to the c axis, i.e., the molecular chain direction. The vapor-deposited OUA11 molecular chains oriented perpendicularly to the substrate, and the films were formed without thermal decomposition for FT-IR spectra. The vapor-deposited OUA11 films showed an incredible surface hardness of 9H because of the high crystallinity and the rigid intermolecular hydrogen bonds. Moreover, the dielectric spectra of the vapor-deposited films suggested that the dipoles of OUA11 were oriented parallel to the substrate because the dielectric constant of the vapor-deposited films was lower than that of the spin-coated films at 123 °C. No peaks of dielectric loss were found for the vapor-deposited films due to the molecular dipole relaxation. The perpendicular vapor-deposited OUA11 films were expected to be low-k materials with a low dielectric constant (2.1–2.3) in the frequency range of 0.1 Hz to 0.1 MHz below 50 °C. The unique structural and electrical properties could not be observed with the spin-coated sample but were found with the vapor-deposited OUA11 sample.

SUPPLEMENTARY MATERIAL

See supplementary materials for FT-IR RAS and transmission spectra of spin-coated OUA11 films (a) in the urea bond vibration region and (b) in the alkyl chain vibration region.

CONFLICTS OF INTEREST

There are no conflicts to declare.

ACKNOWLEDGMENTS

The authors thank Unitika Ltd. for supplying OUA11 and PUA11. This work was partly supported by the MIKIYA Science and Technology Foundation and JSPS KAKENHI.

REFERENCES

[1]. Askari F, Barikani M, Barmar M. (2013) Study on thermal stability of polyurethane-urea based on polysiloxane and polycaprolactone diols. Korean J Chem Eng 30:2093–2099. doi: 10.1007/s11814-013-0139-z.

[2]. Castagna AM, Pangon A, Dillon GP, Runt J. (2013) Effect of Thermal History on the microstructure of a Poly(tetramethylene oxide)-Based Polyurea. Macromolecules 46:6520–6527. doi: 10.1021/ma400856w.

[3]. Morimoto M, Koshiba Y, Misaki M, Ishida K. (2015) Thermal stability of piezoelectric properties and infrared sensor performance of spin-coated polyurea thin films. Appl Phys Express 8. doi: 10.7567/APEX.8.101501.

[4]. Mohotti D, Ngo T, Mendis P, Raman SN. (2013) Polyurea coated composite aluminium plates subjected to high velocity projectile impact. Mater Des 52:1–16. doi: 10.1016/j.matdes.2013.05.060.

[5]. Grujicic M, He T, Pandurangan B, Svingala FR, Settles GS, Hargather MJ. (2012) Experimental characterization and material-model development for microphase-segregated polyurea: an overview. J of Materi Eng and Perform 21:2–16. doi: 10.1007/s11665-011-9875-6.

[6]. Cai L, Al-Ostaz A, Li X, Fowler C, Cheng AH-D, Alkhateb H. (2015) Protection of steel railcar tank containing liquid chlorine from high speed impact by using polyhedral oligomeric silsesquioxane-enhanced polyurea. Int J Implant Eng 75:1–10. doi: 10.1016/j.ijimpeng.2014.06.015.

[7]. Yanase T, Hasegawa T, Nagahama T, Shimada T. (2012) Fabrication of piezoelectric polyurea films by alternating deposition. Jpn J Appl Phys 51:041603.

[8]. Morimoto M, Tsujiura Y, Koshiba Y, Kanno I, Ishida K. (2017) Vibration energy harvester with piezoelectric properties using polyurea thin films. Mol Cryst Liq Cryst 653:188–193. doi: 10.1080/15421406.2017.1351287.

[9]. Tasaka S, Ohta H, Inagaki N. (2000) Nonelectrical poling in ferroelectric polythioureas. IEEE Trans Ultrason Ferroelectr Freq Contr 47:1316–1320. doi: 10.1109/58.883520.

[10]. Kubono A, Murai M, Tasaka S. (2008) High piezoelectric activity in nonpoled thin films prepared by vapor deposition polymerization. Jpn J Appl Phys 47:5553–5557. doi: 10.1143/JJAP.47.5553.

[11]. Morimoto M, Koshiba Y, Misaki M, Ishida K. (2015) Polyurea spin-coated thin films: pyro- and piezoelectric properties and application to infrared sensors. Jpn J Appl Phys 54. doi: 10.7567/JJAP.54.04DK13.

[12]. Tasaka S, Shouko T, Inagaki N. (1992) Ferroelectric Polarization Reversal in Polyureas with Odd Number of CH 2 Groups. Jpn J Appl Phys 31:L1086–L1088. doi: 10.1143/JJAP.31.L1086.

[13]. Tajitsu Y, Ishida K, Kanbara S, Ohigashi H, Date M, Fukada E. (1998) Temperature dependence of switching characteristics in Polyurea-5 Thin Films. Jpn J Appl Phys polyurea-5 37:5375–5378. doi: 10.1143/JJAP.37.5375.

[14]. Hattori T, Takahashi Y, Iijima M, Fukada E. (1996) Piezoelectric and ferroelectric properties of polyurea-5 thin films prepared by vapor deposition polymerization. Journal of Applied Physics polyurea-5 79:1713–1721. doi: 10.1063/1.360959.

[15]. Morimoto M, Koshiba Y, Misaki M, Ishida K. (2015) Structural and electrical characterization of spin-coated polyurea thin films. Polymer (Guildf) 79:128–134.

[16]. Chauhan KV, Sullivan P, Yang JL, Jones TS. (2010) Efficient organic photovoltaic cells through structural modification of chloroaluminum phthalocyanine/fullerene heterojunctions. J Phys Chem C 114:3304–3308. doi: 10.1021/jp910601k.

[17]. Treier M, Richardson NV, Fasel R. (2008) Fabrication of surface-supported low-dimensional polyimide networks. J Am Chem Soc 130:14054–14055. doi: 10.1021/ja805342n.

[18]. Kuwajima S, Horie S, Horiuchi T, Yamada H, Matsushige K, Ishida K. (2009) Crystal and layer structures of ferroelectric oligomer thin films. Macromolecules 42:3353–3357. doi: 10.1021/ma802639r.

[19]. Ueda Y, Ashida M. (1980) The Structure of <italic>n</italic>-Hexatriacontane Film Vacuum-deposited on Alkali Halide Crystals and Its Transformation by Heat

Treatment. J Electron Microsc 29:38–44. doi: 10.1093/oxfordjournals.jmicro.a050206.

[20]. Fukao K, Horiuchi T, Matsushige K. (1989) Observation of molecular orientation in evaporated films of n-paraffins. Thin Solid Films 171:359–366. doi: 10.1016/0040-6090(89)90642-1.

[21]. Tanaka K, Okui N, Sakai T. (1991) Molecular orientation behavior of paraffin thin films made by vapor deposition. Thin Solid Films 196:137–145. doi: 10.1016/0040-6090(91)90181-V.

[22]. Kubono A, Minagawa Y, Ito T. (2009) In situ Observation of Layer-by-Layer Growth in Vapor Deposition of Organic Thin Films. Jpn J Appl Phys 48:020211. doi: 10.1143/JJAP.48.020211.

[23]. Noda K, Ishida K, Horiuchi T, Matsushige K, Kubono A. (1999) Structures of vinylidene fluoride oligomer thin films on alkali halide substrate. Journal of Applied Physics 86:3688–3693. doi: 10.1063/1.371279.

[24]. Nagamatsu S, Kaneto K, Azumi R, Matsumoto M, Yoshida Y, Yase K. (2005) Correlation of the number of thiophene units with structural order and carrier mobility in unsubstituted even- and odd-numbered alpha-oligothiophene films. J Phys Chem B 109:9374–9378. doi: 10.1021/jp044222l.

[25]. Chisaka J, Lu M, Nagamatsu S, Chikamatsu M, Yoshida Y, Goto M, Azumi R, et al. (2007) Structure and electrical properties of unsubstituted oligothiophenes end-capped at the β-position. Chem Mater 19:2694–2701. doi: 10.1021/cm0701658.

[26]. Zhou Y, Taima T, Shibata Y, Miyadera T, Yamanari T, Yoshida Y. (2011) Controlled growth of dibenzotetraphenylperiflanthene thin films by varying substrate temperature for photovoltaic applications. Sol Energy Mater Sol Cells 95:2861–2866. doi: 10.1016/j.solmat.2011.06.001.

[27]. Mitsuta H, Miyadera T, Ohashi N, Zhou Y, Taima T, Koganezawa T, Yoshida Y, et al. (2017) Epitaxial growth of C 60 on rubrene single crystals for a highly ordered organic donor/acceptor interface. Cryst Growth Des 17:4622–4627. doi: 10.1021/acs.cgd.7b00467.

[28]. Meurisch K, Gojdka B, Strunskus T, Zaporojtchenko V, Faupel F. (2012) Vapour phase deposition of highly crystalline self-poled piezoelectric nylon-11. J Phys D: Appl Phys 45:055304. doi: 10.1088/0022-3727/45/5/055304.

[29]. Qian X, Song L, Yu B, Yang W, Wang B, Hu Y, Yuen RKK. (2014) One-pot surface functionalization and reduction of graphene oxide with long-chain molecules: preparation and its enhancement on the thermal and mechanical properties of polyurea. Chem Eng J 236:233–241. doi: 10.1016/j.cej.2013.09.061.

[30]. Li X, Chen D. (2008) Synthesis and characterization of aromatic/aliphatic co-polyureas. J Appl Polym Sci 109:897–902. doi: 10.1002/app.24913.

[31]. Liu S, Cui Z, Zhao Q, Fu P (2014) Piezoelectricity and ferroelectricity in odd-odd nylons with long alkane segments. Appl Phys Lett 104:172906. doi: 10.1063/1.4875017.

[32]. Chonan Y, Matsuba G, Hioki J, Itoh T, Akizuki T (2013) Crystal Structure analysis for polyurea. Proceedings of the 12th Asian Text. Conference 220–223.

[33]. Zhang Q, Mo Z, Zhang H, Liu S, Cheng S. (2001) Crystal transitions of Nylon 11 under drawing and annealing. Polymer (Guildf) 42:5543–5547. doi: 10.1016/S0032-3861(01)00050-7.

[34]. Ohsawa Y, Takahashi R, Maruyama S, Matsumoto Y. (2016) Direct synthesis of porous polyurea films by vapor deposition polymerization in ionic liquid. ACS Macro Lett 5:1009–1013. doi: 10.1021/acsmacrolett.6b00594.

[35]. Busca G, Ramis G, Lorenzelli V, Janin A, Lavalley J-C. (1987) FT-i.r. study of molecular interactions of olefins with oxide surfaces. Spectrochim Acta A Mol Spectrosc 43:489–496. doi: 10.1016/0584-8539(87)80049-1.

[36]. Arnett RL, Crawford BL. (1950) The vibrational frequencies of ethylene. The Journal of Chemical Physics 18:118–126. doi: 10.1063/1.1747428.

[37]. Sanchez Escribano V, Busca G, Lorenzelli V. (1990) Fourier transform infrared spectroscopic studies of the reactivity of vanadia-titania catalysts toward olefins. 1. Propylene. J Phys Chem 94:8939–8945. doi: 10.1021/j100389a017.

[38]. Coleman MM, Sobkowiak M, Pehlert GJ, Painter PC, Iqbal T. (1997) Infrared temperature studies of a simple polyurea. Macromol Chem Phys 198:117–136. doi: 10.1002/macp.1997.021980110.

[39]. Luo, Wang, Ying. (1997) Hydrogen-bonding properties of segmented polyether poly (urethane urea) copolymer. Macromolecules 30:4405–4409. doi: 10.1021/ma951386e.

[40]. Gulmine JV, Janissek PR, Heise HM, Akcelrud L. (2002) Polyethylene characterization by FTIR. Polym Test 21:557–563. doi: 10.1016/S0142-9418(01)00124-6.

[41]. Abe K, Sakurai H. (2006) A trend of low dielectric constant materials. Kobunshi 55:82–85. doi: 10.1295/kobunshi.55.82.

[42]. Yokoyama D, Saito H, Kitai Y, Fujiwara H, Inagaki K. (2012) Developing thermosetting resin system with low molecular weight PPE to achieve lower dielectric property. J Netw Polym (Japanese) 33:336–340. doi: 10.11364/networkpolymer.33.336.

[43]. Nguyen CV, Carter KR, Hawker CJ, Hedrick JL, Jaffe RL, Miller RD, Remenar JF, et al. (1999) Low-dielectric, nanoporous organosilicate films prepared via inorganic/organic polymer hybrid templates. Chem Mater 11:3080–3085. doi: 10.1021/cm990114d.

[44]. Volksen W, Miller RD, Dubois G. (2010) Low dielectric constant materials. Chem Rev 110:56–110. doi: 10.1021/cr9002819.

[45]. Maier G. (2001) Low dielectric constant polymers for microelectronics. Prog Polym Sci 26:3–65. doi: 10.1016/S0079-6700(00)00043-5.